## PAPER

Check for updates

# Cobalt doped graphitic carbon nitride as an effective catalyst for peracetic acid to degrade sulfamethoxazole†

Runyu Zhou, Gaofeng Zhou, Yiqing Liu, [ID] * Shixiang Wang and Yongsheng Fu*

In this study, cobalt doped graphitic carbon nitride (Co–CN) was prepared and applied as a catalyst to activate peracetic acid (PAA) for sulfamethoxazole (SMX) degradation at neutral pH. PAA could be efficiently activated by Co–CN resulting in the efficient degradation of SMX. Characterization results of fresh and used Co–CN suggested that cobalt was successfully doped in graphitic carbon nitride (g-$C_3N_4$) through chemical bonding (Co–N bond) and the surface cobalt species in Co–CN (*i.e.*, $\equiv$Co(II) and $\equiv$Co(III)) were the main activators for PAA. Organic radicals (*i.e.*, $CH_3C(O)O^{\bullet}$ and $CH_3C(O)OO^{\bullet}$) were proved to be the dominant reactive species for SMX removal in the Co–CN/PAA system by radical scavenging experiments. The increase of cobalt doping content, PAA dosage or Co–CN dosage could accelerate SMX degradation and the neutral condition was highly favorable to SMX removal in Co–CN/PAA system. Co–CN exhibited a good stability and reusability for PAA activation in degrading SMX. Four possible degradation pathways of SMX (*i.e.*, hydroxylation, nitration, bond cleavage and coupling reaction) were proposed in the Co–CN/PAA system according to eight identified transformation products.

## 1. Introduction

Nowadays, antibiotics are widely used in the aquaculture, breeding and medicinal fields to treat and prevent bacterial infections.[1] With their widespread use, more and more antibiotics and their by-products have been discharged into the environment through industrial effluents and sewage effluents.[2] Therefore, water pollution caused by these emerging contaminants is gaining more and more attention due to their potential risk on aquatic organisms and human health. Sulfamethoxazole (SMX), a common sulfonamide antibiotic, is widely used in treating infectious diseases.[3] Since it cannot be completely removed in conventional wastewater treatment plants, it has been frequently detected in ground water and surface water.[4] Thus, it is essential to develop environmentally friendly technologies with high efficiency and low cost to remove SMX from wastewater. Up till now, advanced oxidation processes (AOPs) have drawn great attention in the disposal of SMX-containing wastewater due to their excellent performance.[5,6] Reactive oxygen species (ROS), such as hydroxyl radical ($^{\bullet}OH$),[7] sulfate radical ($SO_4^{\bullet-}$)[8] and organic radicals (R–O$^{\bullet}$)[9,10] generated through the activation of different precursors in AOPs, are mainly responsible for the elimination and mineralization of SMX.

As a widely used disinfectant in textile, medical industries and wastewater treatment, peracetic acid (PAA, $CH_3C(O)OOH$) has attracted an increased interest in AOPs as an alternative precursor recently. The O–O bond in PAA possesses a lower bond energy (159 kJ mol$^{-1}$) than that in peroxymonosulfate (PMS, 317 kJ mol$^{-1}$) or hydrogen peroxide ($H_2O_2$, 213 kJ mol$^{-1}$),[11] which makes PAA activation more easily. PAA can be activated by UV radiation,[12] thermal activation[13] and transition metals.[7,14] Among these activators, transition metal is regarded as the most cost-effective and energy-efficient candidate because of its abundant natural abundance, excellent catalytic performance and low cost.[15] There are several publications on removing SMX by PAA activation with transition metals. For instance, Wang *et al.*[2] reported that PAA could be activated by Fe$^{2+}$-zeolite to produce $^{\bullet}OH$, leading to an efficient SMX removal. Kim *et al.*[9] found that PAA could be efficiently activated by Co(II) resulting in a high removal efficiency of SMX.

Compared with other transition metals (*e.g.*, Cu, Fe and Mn), cobalt shows much more efficient catalytic performance on PAA activation.[11,16,17] Wang *et al.*[11] reported that in Co(II)/PAA system, an extremely low dosage of Co(II) (lower than 1 μM) could induce 99.9% SMX removal. However, homogeneous cobalt ion activation systems will result in a secondary pollution to aquatic environment due to the potential toxicity of cobalt ion.[14] As a result, cobalt-based heterogeneous catalysts have been proposed in PAA systems to overcome the shortcomings induced by homogeneous cobalt ion, such as cobaltosic oxide ($Co_3O_4$),[14] cobalt ferrite ($CoFe_2O_4$)[18] and lanthanum cobaltite perovskite ($LaCoO_3$).[19] However, the above cobalt-based

*Faculty of Geosciences and Environmental Engineering, Southwest Jiaotong University, Chengdu 611756, China. E-mail: liuyq@swjtu.edu.cn; fuyosh@163.com*

† Electronic supplementary information (ESI) available. See https://doi.org/10.1039/d2ra00821a

heterogeneous catalysts possess unsatisfactory catalytic efficiency and poor dispersibility in aqueous solution with inevitable leaching of cobalt ion. Therefore, it is essential to find a proper way that can promote the catalytic efficiency and restrain the leaching of cobalt ion to improve the cobalt-based catalysts.

Graphitic carbon nitride (g-C$_3$N$_4$) has been widely used in photocatalysis, biological sensing and other fields due to its high stability, chemical versatility, electron-rich structure and nontoxicity.[20–22] The unique structural and electronic properties of g-C$_3$N$_4$ can be attributed to the heptazine rings with pyridinic nitrogen groups in g-C$_3$N$_4$ in which the six nitrogen lone pairs can serve as electron donors.[23] Hence, g-C$_3$N$_4$ has an impressive capability to entrap metal ions through metal–N interaction. G-C$_3$N$_4$ can provide a versatile platform to immobilize metal catalysts in its framework, which can restrain the leaching of metal ion and promote its internal charge transfer.[23,24] As a result, cobalt doped g-C$_3$N$_4$ (Co–CN) has been developed to apply as a catalyst in AOPs.[25,26] For instance, Xie *et al.*[25] reported that Co–CN could activate PMS leading to monochlorophenols degradation. Yang *et al.*[21] prepared Co–CN nanosheet as a photocatalyst to degrade methylene blue, which obtained an excellent treatment efficiency. However, research on the application of Co–CN in PAA-based AOPs is extremely limited. Herein, in order to achieve an efficient catalytic performance and control the leaching of cobalt ion, Co–CN was synthesized for PAA activation to degrade SMX in this study.

The main objectives of this work were to: (1) explore the feasibility and mechanism of PAA activation by Co–CN; (2) identify the dominant reactive species for SMX removal in Co–CN/PAA system; (3) investigate the effects of different operational factors on SMX degradation; (4) evaluate the stability and reusability of Co–CN for PAA activation in degrading SMX; and (5) propose the possible degradation pathways of SMX in Co–CN/PAA system.

## 2. Material and methods

### 2.1 Chemicals

All the chemicals used in this work are shown in Text S1 in the ESI.†

### 2.2 Catalysts synthesis and characterization

Co–CN was synthesized through a facile calcination method,[25] and the detailed synthesis processes are described in Text S2.† For comparison, pure g-C$_3$N$_4$[26] and cobalt oxide[27] were synthesized through the same way in the absence of Co(NO$_3$)$_2$·6H$_2$O and urea, respectively. Additionally, to evaluate the effect of cobalt doping content in Co–CN on SMX removal, Co–CN with different cobalt doping contents were also synthesized by adding 0.05, 0.1, 0.15, 0.2 and 0.5 g of Co(NO$_3$)$_2$·6H$_2$O, respectively, which were denoted as Co–CN-$x$ ($x$ = 0.5, 1, 1.5, 2 and 5, respectively). Unless otherwise noted, Co–CN represented cobalt doped g-C$_3$N$_4$ with the corresponding Co(NO$_3$)$_2$·6H$_2$O dosage of 0.2 g.

The prepared pure g-C$_3$N$_4$, cobalt oxide, fresh Co–CN and used Co–CN were characterized by the X-ray diffraction (XRD), X-ray photoelectron spectroscope (XPS) and scanning electron microscope (SEM) coupled with an energy diffraction spectrum (EDS), and the detailed characterization information is shown in Text S3†.

### 2.3 Experimental procedure

All the experiments were carried out in a 250 mL glass reactor with constant mechanical stirring at 25 °C in a thermostatic magnetic bath. Designated concentration of PAA and 5 μM SMX were firstly added into the reactor, respectively. Then, the initial pH of reaction solution was adjusted by 0.1 M H$_2$SO$_4$ and 0.1 M NaOH to the predetermined value. Finally, the reaction was initiated as Co–CN was added into the above solution. 1 mL of supernatant was collected at specific time intervals, mixed with excess Na$_2$S$_2$O$_3$ for quenching residual oxidants, and filtered through 0.22 μm polytetrafluoroethylene membrane for further analysis. 50 mM methanol (MeOH) or 50 mM tert-butanol (TBA) was introduced into the reaction solution before adding Co–CN in radical scavenging experiments. For the study on reusability of Co–CN, the used Co–CN was recovered with filtration and washed with deionized water for five times to eliminate the residual SMX and reactive species before drying in vacuum at 60 °C overnight. Then, the obtained used Co–CN was again applied to SMX degradation in the same conditions. All of the experiments were conducted at least twice to minimize the error.

### 2.4 Analysis

Detailed information about analyses of SMX concentration and its transformation products are shown in Text S4.† The PAA concentration was regularly calibrated using a colorimetric method.[28] The pH value of reaction solution was measured using a pH meter (PHS-3C, Leici, China). The concentration of leached cobalt ion was quantified by an inductively coupled plasma mass spectrometer (ICP-MS, Agilent ICPMS 7700, USA). The degradation of SMX in Co–CN/PAA system followed a pseudo first-order kinetic model and the observed rate constant ($k_{obs}$) of SMX degradation was thus calculated *via* eqn (1).

$$\ln\left(\frac{C_0}{C_t}\right) = k_{obs}t \qquad (1)$$

where $C_0$ and $C_t$ refer to the concentrations of SMX at initial time and reaction time $t$, respectively.

## 3. Results and discussion

### 3.1 Degradation of SMX by Co–CN/PAA

The SMX removal in various systems were investigated and the results are shown in Fig. 1. In Co–CN alone system, no SMX removal was observed, indicating the negligible adsorption of Co–CN for SMX. Since the oxidation capacity of PAA was weak, only 6.2% SMX was removed by PAA alone. However, the combination of Co–CN and PAA could induce an efficient degradation of SMX, which was probably due to that PAA was activated by Co–CN leading to the generation of reactive species.
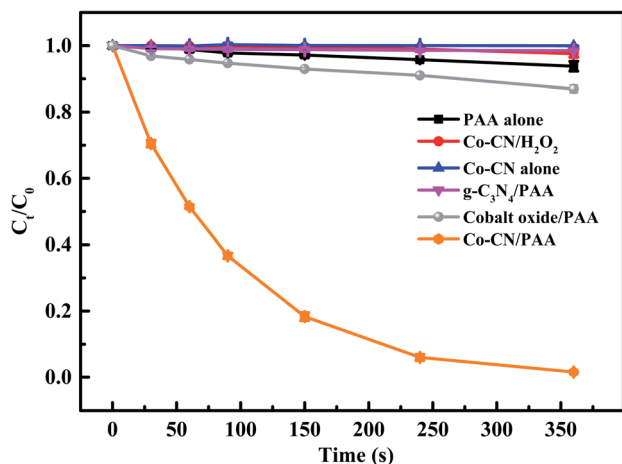
**Fig. 1** Degradation of SMX in different systems. Experimental conditions: $[PAA]_0 = 0.1$ mM, $[H_2O_2]_0 = 0.24$ mM, $[Co-CN]_0 = [g-C_3N_4]_0 = [cobalt\ oxide]_0 = 50$ mg $L^{-1}$, $[SMX]_0 = 5$ μM, $pH_0 = 6.5$, $T = 25$ °C.

Negligible SMX removal was observed in g-$C_3N_4$/PAA system, which indicated the ineffective activation of g-$C_3N_4$ to PAA. Besides, the cobalt oxide was used to remove SMX with the combination of PAA, aiming to evaluate its feasibility on PAA activation in Co–CN/PAA system, and only 13.1% SMX removal was observed in cobalt oxide/PAA system. These results indicated that, as the thermal decomposition products of urea and $Co(NO_3)_2 \cdot 6H_2O$, respectively, g-$C_3N_4$ and cobalt oxide were unable to efficiently activate PAA. Since commercial PAA solution consists of PAA and $H_2O_2$, to clarify if $H_2O_2$ contributed to the SMX degradation in Co–CN/PAA system, SMX removal in Co–CN/$H_2O_2$ system was investigated. As depicted in Fig. 1, a negligible SMX removal was observed in Co–CN/$H_2O_2$ system, indicating that $H_2O_2$ played a negligible role in Co–CN/PAA system.

Generally, the ineluctable leaching of metal ions in metal-based heterogeneous systems can occur and the leached metal ions may also participate in the activation of peroxides through homogeneous processes synchronously.[18,29] Therefore, the concentration of leached cobalt ion in Co–CN/PAA system was determined, which was 18 μg $L^{-1}$ after reaction. To evaluate the possible contribution of leached cobalt ion to SMX removal, $Co^{2+}$/PAA system was used to degrade SMX at selected dosage of $[Co^{2+}] = 20$ μg $L^{-1}$. As shown in Fig. S2,† 49.6% SMX was removed within 360 s, which was significantly lower than that in Co–CN/PAA system (98.5%). Since the concentration of leached cobalt ion in SMX degradation process by Co–CN/PAA was lower than the final measured concentration, the actual contribution of leached cobalt ion to SMX removal was probably lower than that in $Co^{2+}$/PAA system. Hence, the heterogeneous catalysis process dominantly contributed to SMX removal in Co–CN/PAA system. Similar results were also found in previous cobalt-based heterogeneous systems.[14,25,30]

### 3.2 PAA activation mechanism by Co–CN

**3.2.1 Characterization of catalyst.** The XRD patterns of cobalt oxide, g-$C_3N_4$ as well as fresh and used Co–CN were

detected and are shown in Fig. 2. In the XRD pattern of cobalt oxide, peaks at $2\theta = 19.1°$, $31.4°$, $36.9°$, $38.7°$, $44.9°$, $55.8°$, $59.5°$ and $65.4°$ were well assigned to the (1 1 1), (2 2 0), (3 1 1), (2 2 2), (4 0 0), (4 2 2), (5 1 1) and (4 4 0) facets of $Co_3O_4$, respectively (PDF#74-1656), indicating that the cobalt oxide was $Co_3O_4$. The diffraction peaks at $12.9°$ and $27.2°$ in the XRD pattern of g-$C_3N_4$, corresponding to the (1 0 0) and (0 0 2) crystal planes of g-$C_3N_4$, were indexed to the tri-$s$-triazine units and conjugated aromatic segments in g-$C_3N_4$, respectively.[31] However, compared with pure g-$C_3N_4$, peaks corresponding to the (1 0 0) and (0 0 2) crystal planes of g-$C_3N_4$ in fresh Co–CN shifted slightly to a higher angle and their intensities decreased significantly, indicating the decrease of stacking distance between g-$C_3N_4$ layers.[21] The above results suggested that although the main structure of g-$C_3N_4$ was maintained after the introduction of cobalt, the polymeric condensation of g-$C_3N_4$ might be influenced.[32] Moreover, no characteristic peak of $Co_3O_4$ or other cobalt compounds (e.g., cobalt nitrides and cobalt carbides) was observed in the XRD pattern of fresh Co–CN, suggesting that cobalt might be incorporated in the framework of g-$C_3N_4$ and possessed a highly dispersive distribution.[32,33] Compared with fresh Co–CN, the XRD pattern of used Co–CN had little change. This result suggested that the crystal structure of Co–CN was unchanged during reaction with PAA and Co–CN possessed a good structural stability.

To clarify the chemical composition of Co–CN, XPS survey was introduced. In the survey spectrum of fresh Co–CN (Fig. 3a), peaks of C, N, Co and inevitable O were observed. In C 1s spectrum of fresh Co–CN (Fig. 3b), peaks at 284.8 and 288.3 eV were assigned to C–C and N–C=N in triazine ring unites of g-$C_3N_4$, respectively.[34] The N 1s spectrum of fresh Co–CN (Fig. 3c) showed two peaks at 398.7 and 401.2 eV, which were characteristic peaks of C–N=C and H–N–$C_2$ in g-$C_3N_4$, respectively.[35,36] The above results further confirmed that the triazine units of g-$C_3N_4$ were conserved in Co–CN during the synthesis process. Furthermore, in N 1s spectrum of fresh Co–CN, peak at 399.9 eV was characteristic peak of Co–N bond, suggesting that chemical
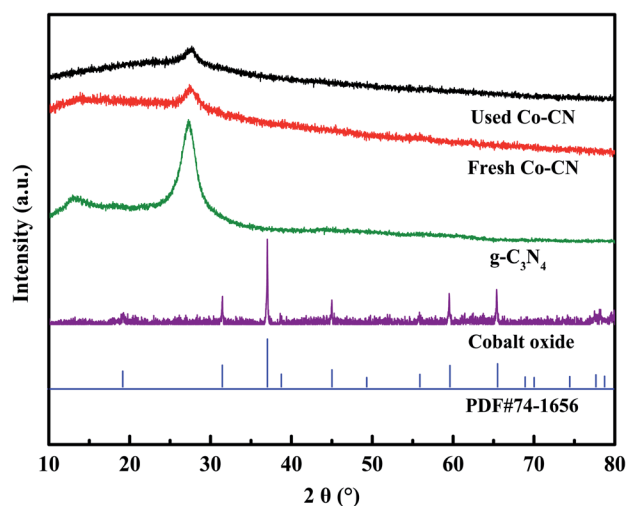


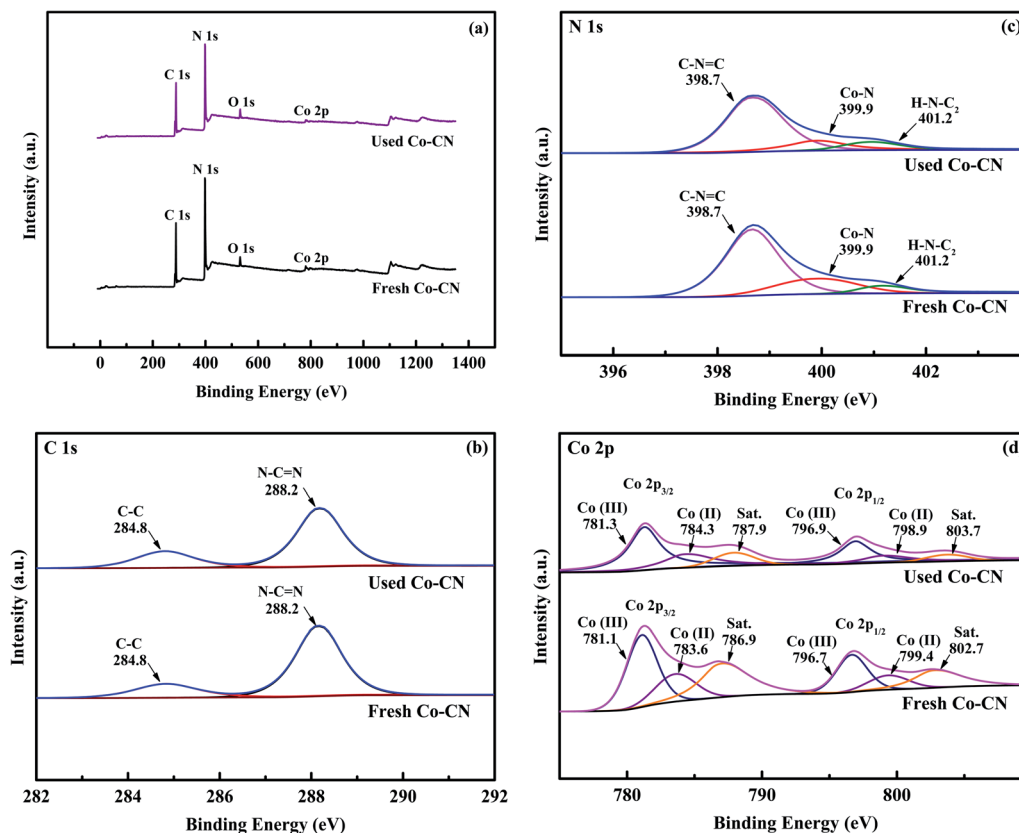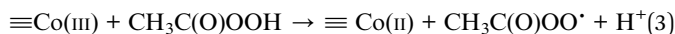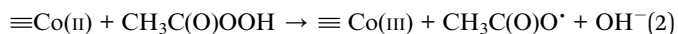**Fig. 2** XRD patterns of cobalt oxide, g-$C_3N_4$, fresh and used Co–CN.

**Fig. 3** XPS spectra of fresh and used Co–CN: survey spectrum (a), C 1s (b), N 1s (c) and Co 2p (d).

bonding between cobalt and g-C$_3$N$_4$ in Co–CN was an important pathway for their combination.[36] Finally, as shown in Fig. 3d, two peaks at 781.3 and 796.8 eV in Co 2p spectrum of fresh Co–CN could be assigned to Co 2p$_{3/2}$ and Co 2p$_{1/2}$, respectively, while peaks at 786.9 and 802.7 eV were the corresponding shake-up satellite peaks. Two characteristic peaks at 781.1 and 796.7 eV were attributed to $\equiv$Co(III), and peaks at 783.6 and 799.4 eV referred to $\equiv$Co(II).[18]

For comparison, the XPS spectrum of used Co–CN was also investigated. Little change was observed in C 1s and N 1s spectra of used Co–CN (Fig. 3b and c), indicating that triazine units in g-C$_3$N$_4$ and the chemical bonding between cobalt and g-C$_3$N$_4$ in Co–CN were well conserved after reaction. In the Co 2p spectrum of used Co–CN, similar characteristic peaks could still be observed, while the intensities of these peaks decreased compared to those in fresh Co–CN. This might be due to the loss of doped cobalt during reaction. The $\equiv$Co(II)/$\equiv$Co(III) ratio in fresh Co–CN was 0.48, which decreased to 0.39 in used Co–CN. This variation indicated that the $\equiv$Co(II) in Co–CN could take part in PAA activation (eqn (2)). However, after reaction with PAA, the decrease of $\equiv$Co(II)/$\equiv$Co(III) ratio in Co–CN was only 0.09, which indicated that the reduction of $\equiv$Co(III) (eqn (3)) was synchronously existed during PAA activation, resulting in the redox cycle of $\equiv$Co(II)/$\equiv$Co(III).[14]

$$\equiv\text{Co(II)} + CH_3C(O)OOH \rightarrow\ \equiv Co\text{(III)} + CH_3C(O)O^{\bullet} + OH^{-}\quad(2)$$

$$\equiv\text{Co(III)} + CH_3C(O)OOH \rightarrow\ \equiv Co\text{(II)} + CH_3C(O)OO^{\bullet} + H^{+}\quad(3)$$

The morphologies of g-C$_3$N$_4$, cobalt oxide as well as Co–CN before and after reaction recorded by SEM. As shown in Fig. 4a, a coral porous structure with large dispersive nanopores was observed in SEM image of g-C$_3$N$_4$. Cobalt oxide, which was proved to be Co$_3$O$_4$ by XRD pattern, displayed a large amount of agglomerated particles in Fig. 4b. As shown in Fig. 4c, the coral porous structure of g-C$_3$N$_4$ could still be observed in fresh Co–CN, suggesting that the basic morphology of g-C$_3$N$_4$ was conserved in fresh Co–CN. However, the porous structure in fresh Co–CN got a tighter distribution than that in g-C$_3$N$_4$, which might be due to the decrease of stacking distance between g-C$_3$N$_4$ layers caused by the introduction of cobalt into g-C$_3$N$_4$.[21,25] No morphology of Co$_3$O$_4$ or other cobalt species was observed in SEM image of fresh Co–CN, indicating again that cobalt was incorporated into g-C$_3$N$_4$ rather than forming a simple mixture of Co$_3$O$_4$ and g-C$_3$N$_4$. The above results were consistent with XRD and XPS analyses. In addition, the corresponding element mappings of fresh Co–CN showed the uniform distribution of cobalt element in carbon and nitrogen elements, indicating that cobalt was evenly distributed in the structure of g-C$_3$N$_4$, which could serve as abundant active sites for the activation of PAA. For comparison, the morphology of used Co–CN was also recorded by SEM (Fig. 4d), and no obvious morphological change was observed in used Co–CN. Besides, the uniform distribution of cobalt element was still observed in
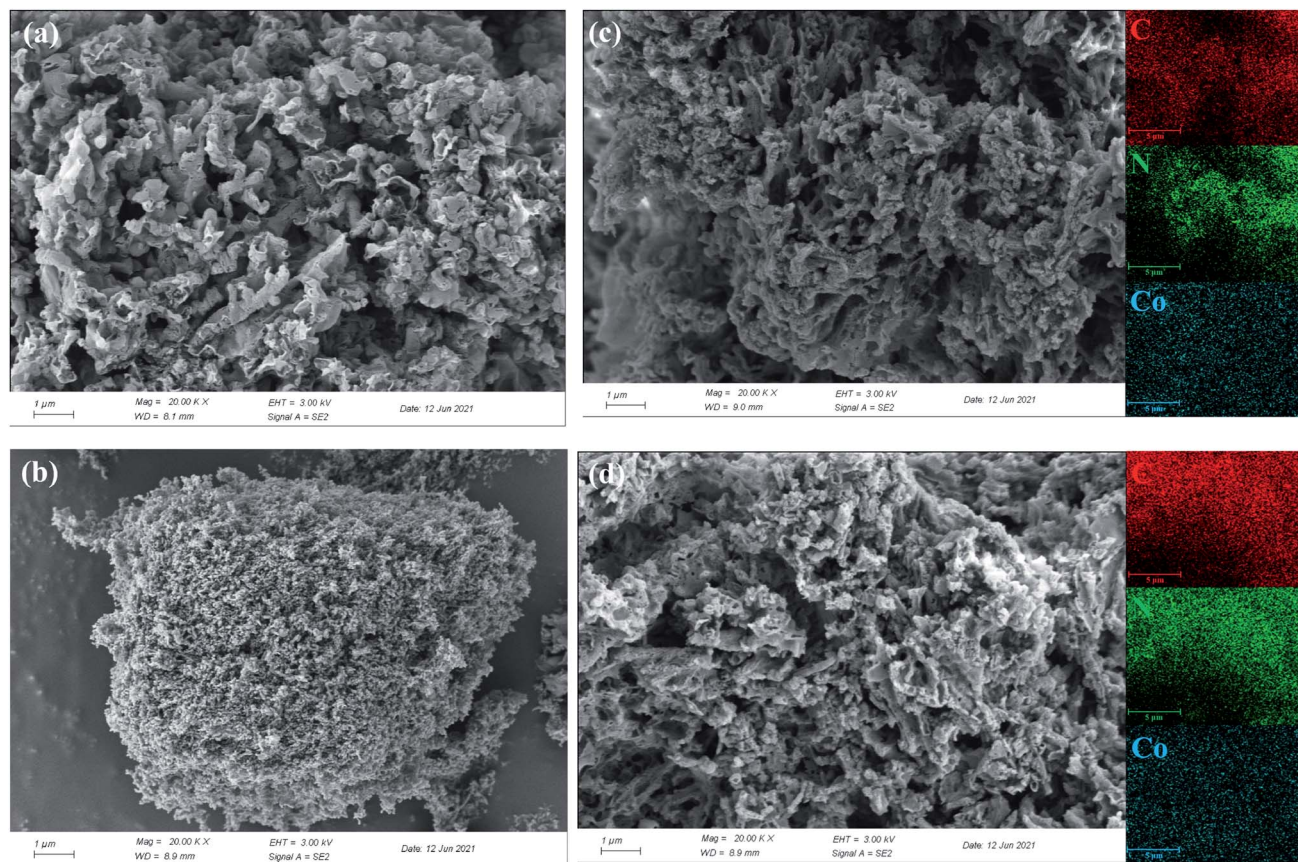
**Fig. 4** SEM images of g-$C_3N_4$ (a), cobalt oxide (b), fresh Co–CN (c), used Co–CN (d) and the corresponding element mappings of C, N and Co.

the corresponding element mapping of used Co–CN, indicating that the used Co–CN could still anchor cobalt with good stability and uniform distribution. These results further confirmed the good structural stability of Co–CN.

Besides, the specific surface areas of g-$C_3N_4$ and Co–CN were determined by Brunauer–Emmett–Teller (BET) analysis through $N_2$ adsorption/desorption isotherms as well as Barrett–Joyner–Halenda (BJH) method. As exhibited in Fig. S3,† the BET surface areas of g-$C_3N_4$ and Co–CN were determined to be 40.77 and 61.36 $m^2$ $g^{-1}$, respectively. This result indicated that the introduction of cobalt could enlarge the specific surface area of g-$C_3N_4$, which was favorable to supply abundant active sites for PAA activation.

**3.2.2 Identification of reactive species in Co–CN/PAA system.** Except for $CH_3C(O)O^{\bullet}$ and $CH_3C(O)OO^{\bullet}$ produced *via* eqn (2) and (3), subsequent radical reactions would produce other reactive species in PAA-based AOPs, such as $^{\bullet}CH_3$ and $CH_3OO^{\bullet}$ (eqn (4) and (5)).[2,9,11] However, their contribution to SMX removal in Co–CN/PAA system could be ignored because of their weaker oxidation capacity.[11] To confirm this speculation, $N_2$ was pumped into the reaction solution for 30 min to eliminate the dissolved oxygen (DO) in the solution before the reaction initiated. Because $^{\bullet}CH_3$ can react with DO to form $CH_3OO^{\bullet}$ (eqn (5)), the contribution of $^{\bullet}CH_3$ and $CH_3OO^{\bullet}$ could be distinguished when DO was excluded from the reaction solution. As shown in Fig. S4,† the purging of $N_2$ had a negligible

impact on SMX removal in Co–CN/PAA system, indicating that the role of $^{\bullet}CH_3$ and $CH_3OO^{\bullet}$ to SMX degradation could be ignored.[19] Besides, $^{\bullet}OH$ was proved to be absent in reported cobalt-based PAA systems.[9,11,14] Thus, the dominant reactive species for SMX removal in Co–CN/PAA system might be $CH_3C(O)O^{\bullet}$ and $CH_3C(O)OO^{\bullet}$. Radical scavenging experiments utilizing scavengers (*i.e.*, TBA and MeOH) were conducted to further validate the absence of $^{\bullet}OH$ and the contribution of $CH_3C(O)O^{\bullet}$ and $CH_3C(O)OO^{\bullet}$ to SMX removal in Co–CN/PAA system. TBA could selectively quench $^{\bullet}OH$ ($k_{TBA/^{\bullet}OH} = 6 \times 10^8$ $M^{-1}$ $s^{-1}$),[11,37] whereas both $^{\bullet}OH$ ($k_{MeOH/^{\bullet}OH} = 6 \times 10^8$ $M^{-1}$ $s^{-1}$)[11] and organic radicals (R–$O^{\bullet}$, *i.e.*, $CH_3C(O)O^{\bullet}$ and $CH_3C(O)OO^{\bullet}$) could be efficiently quenched by MeOH. In spite of the fact that the second-order rate constant between MeOH and R–$O^{\bullet}$ is unknown, previous studies had proved that MeOH could efficiently scavenge R–$O^{\bullet}$.[11,37] As shown in Fig. 5, the presence of TBA had a negligible impact on SMX degradation in Co–CN/PAA system, which indicated that $^{\bullet}OH$ was indeed not generated in this system. However, the presence of MeOH inhibited 74.4% SMX degradation, and the corresponding degradation rate constant of SMX declined from 0.0113 $min^{-1}$ in Co–CN/PAA system to 0.0011 $min^{-1}$ in Co–CN/PAA/MeOH system. These results demonstrated that in Co–CN/PAA system, R–$O^{\bullet}$ (*i.e.*, $CH_3C(O)O^{\bullet}$ and $CH_3C(O)OO^{\bullet}$) was the dominant reactive species responsible for the degradation of SMX. Similar results were also found in previous publications.[14,18,19]
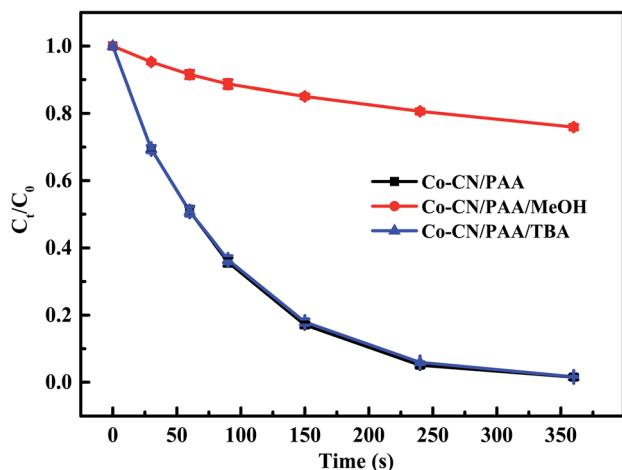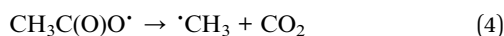
Fig. 5 Effect of radical scavengers on SMX removal. Experimental conditions: $[PAA]_0 = 0.1$ mM, $[TBA]_0 = [MeOH]_0 = 50$ mM, $[catalyst]_0 = 50$ mg L$^{-1}$, $[SMX]_0 = 5$ μM, $pH_0 = 6.5$, $T = 25$ °C.

$$CH_3C(O)O^\bullet \rightarrow {}^\bullet CH_3 + CO_2 \qquad (4)$$

$$^\bullet CH_3 + O_2 \rightarrow CH_3OO^\bullet \qquad (5)$$

**3.2.3 Mechanism of PAA activation.** The aforementioned characterization results revealed that cobalt was distributed evenly in Co–CN through chemical bonding (Co–N bond). The surface $\equiv$Co(II) and $\equiv$Co(III) in Co–CN could react with PAA to generate radical species, and R–O$^\bullet$ (i.e., $CH_3C(O)O^\bullet$ and $CH_3C(O)OO^\bullet$) was proved to be the dominant reactive species responsible for the degradation of SMX in Co–CN/PAA system. Therefore, a plausible PAA activation mechanism by Co–CN was proposed in Fig. 6. At first, the surface $\equiv$Co(II) gave an electron to PAA, yielding $CH_3C(O)O^\bullet$ and $\equiv$Co(III) (eqn (2)). Subsequently, the surface $\equiv$Co(III) could also react with PAA to generate $CH_3C(O)OO^\bullet$, synchronously producing $\equiv$Co(II) to constitute the redox cycle of $\equiv$Co(II)/$\equiv$Co(III) (eqn (3)).
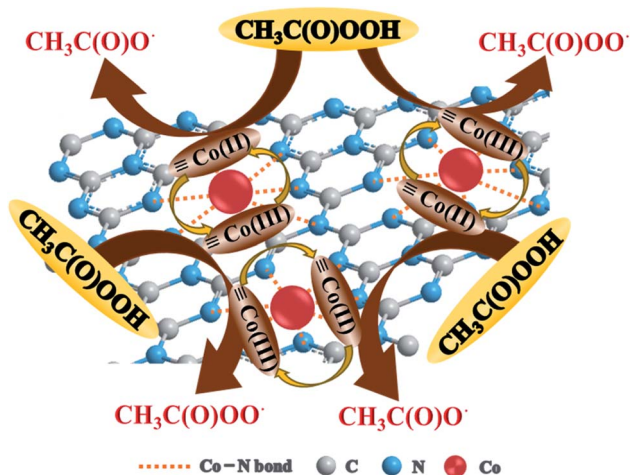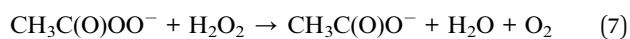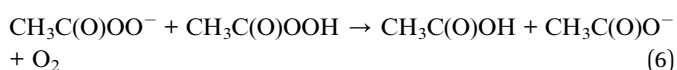


Fig. 6 The possible mechanism for PAA activation by Co–CN.

### 3.3 Factors influencing SMX degradation by Co–CN/PAA

**3.3.1 Effect of cobalt doping content.** Since cobalt doping content could significantly affect the catalytic activity of Co–CN,[25] Co–CN composites with different cobalt doping content were used to evaluate their catalytic performances on SMX removal. As shown in Table S1,† the weight percentage of cobalt in Co–CN measured by EDS enhanced from 2.38% to 22.53% when the dosage of $Co(NO_3)_2 \cdot 6H_2O$ increased from 0.05 to 0.5 g. As presented in Fig. 7a, with increasing cobalt doping content in Co–CN, the SMX removal efficiency in Co–CN/PAA system increased from 51.7% to 99%, and the corresponding $k_{obs}$ within 240 s enhanced from 0.0021 to 0.015 min$^{-1}$. The increase of cobalt doping content in Co–CN could provide more active sites for the activation of PAA yielding more reactive species in Co–CN/PAA system, which resulted in the enhanced degradation of SMX. Since Co–CN with the corresponding $Co(NO_3)_2 \cdot 6H_2O$ dosage of 0.2 g (Co–CN-2) had already reached an excellent SMX removal, it was selected as the recommended catalyst in this study.

**3.3.2 Effect of initial pH.** As shown in Fig. 7b, the effect of initial pH on SMX removal by Co–CN/PAA was investigated. The optimal pH for SMX removal in Co–CN/PAA system was at pH 6.5 and 98.5% SMX was removed in 360 s. However, the $k_{obs}$ of SMX degradation in Co–CN/PAA system within 240 s under alkaline and strongly acidic conditions were much lower than that at pH 6.5, indicating that alkaline and strongly acidic conditions were unfavorable to SMX removal. Since the pKa of PAA is around 8.2, PAA was mainly existed as neutral form ($CH_3C(O)OOH$) in acidic condition, as depicted in Fig. S5,† and it was too stable to be activated easily. Besides, acidic condition with a high concentration of H$^+$ would restrain the generation of $CH_3C(O)OO^\bullet$ (eqn. (3)),[11] which might affect the degradation of SMX in Co–CN/PAA system. At alkaline conditions (pH 9.5 and 11.0), PAA was mainly existed as the deprotonated form ($CH_3C(O)OO^-$) and it could be rapidly decomposed via eqn (6) and (7).[11] The rapid decomposition of PAA in alkaline condition would cut down the generation of reactive species and subsequently suppress SMX removal in Co–CN/PAA system. As a result, pH 6.5 was the optimal condition for SMX removal in Co–CN/PAA system.

$$CH_3C(O)OO^- + CH_3C(O)OOH \rightarrow CH_3C(O)OH + CH_3C(O)O^- + O_2 \qquad (6)$$

$$CH_3C(O)OO^- + H_2O_2 \rightarrow CH_3C(O)O^- + H_2O + O_2 \qquad (7)$$

**3.3.3 Effect of PAA dosage.** PAA dosage can affect not only the removal efficiency of SMX but also the treatment cost of this system. As exhibited in Fig. 7c, when the molar ratio of PAA/SMX increased from 50 to 300 in Co–CN/PAA system, the degradation efficiency of SMX enhanced from 78.7% to 100% and the corresponding $k_{obs}$ within 240 s gradually increased from 0.0048 to 0.0165 min$^{-1}$, which might be due to the generation of more reactive species with increasing PAA dosage. Similar result was also reported in the degradation of SMX in $CoFe_2O_4$/PAA system.[18] Considering the treatment efficiency of
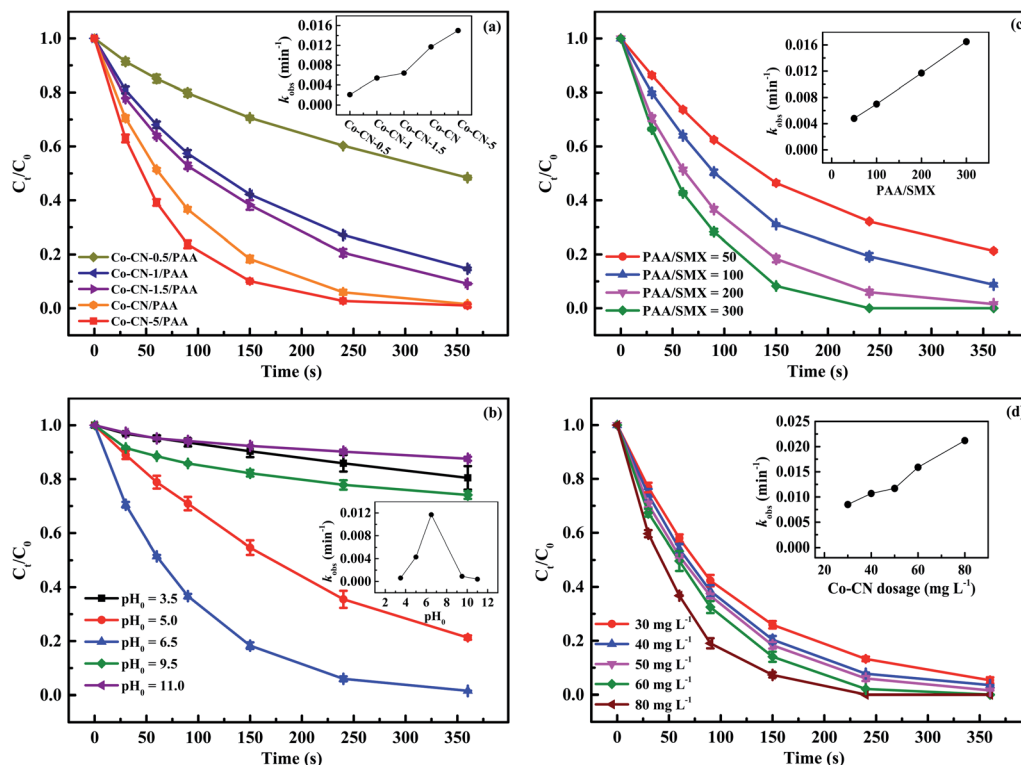
**Fig. 7** Effects of cobalt doping content (a), initial pH (b), PAA dosage (c) and Co−CN dosage (d) on SMX removal. The inserts are the $k_{obs}$ of SMX degradation in Co−CN/PAA system under different conditions. Experimental conditions: $[PAA]_0 = 0.1$ mM except (c), $[catalyst]_0 = 50$ mg L$^{-1}$ except (d), $[SMX]_0 = 5$ μM, $pH_0 = 6.5$ except (b), $T = 25$ °C.

SMX and operation cost comprehensively, the molar ratio of PAA/SMX was recommended to be 200 in this work, because SMX was nearly removed within 360 s in this molar ratio of PAA/SMX.

**3.3.4 Effect of Co−CN dosage.** The effect of Co−CN dosage on SMX degradation in Co−CN/PAA system was also investigated and the results are shown in Fig. 7d. When the Co−CN dosage increased from 30 to 80 mg L$^{-1}$, the SMX degradation efficiency increased gradually and the corresponding $k_{obs}$ within 240 s enhanced from 0.0085 to 0.0212 min$^{-1}$. Increasing Co−CN dosage could provide more active sites for the activation of PAA, which would yield more reactive species in Co−CN/PAA system. Therefore, SMX removal enhanced gradually with increasing Co−CN dosage in this system. Similar phenomenon was also observed in Co$_3$O$_4$/PAA system.[14,19]

## 3.4 Stability and reusability of Co−CN

To investigate the stability and reusability of Co−CN, three continuous runs on SMX degradation using the recycled catalyst were conducted. As shown in Fig. 8, the SMX removal efficiency in each run was 98.5%, 98.4% and 97.7%, respectively, indicating that Co−CN possessed an excellent reusability for PAA activation. This could be explained that there was a strong interconversion between $\equiv$Co(II) and $\equiv$Co(III) in Co−CN through eqn (2) and (3) providing plenty of active sites in Co−CN for PAA activation. Besides, the existence of Co−N bond in Co−

CN contributed to anchoring cobalt in the structure of Co−CN and preventing the loss of active sites in Co−CN during the reuse process.[10] Additionally, little change was observed in the XRD pattern and SEM image of used Co−CN, which also implied a good stability of Co−CN. Combined with the above results, Co−CN was considered to have a good stability and reusability for PAA activation in degrading SMX.
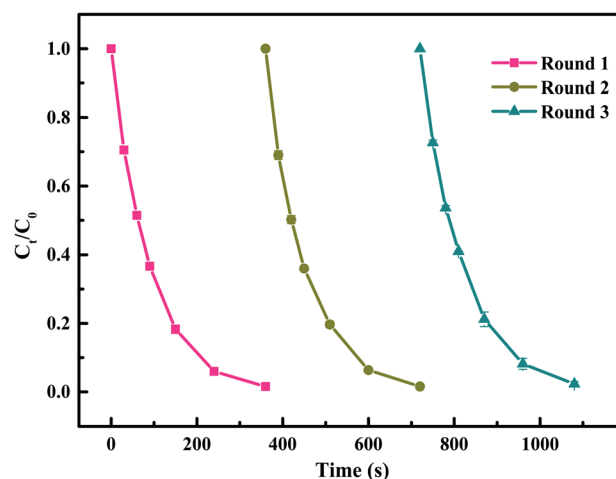


**Fig. 8** Reusability of Co−CN on PAA activation for SMX degradation. Experimental conditions: $[PAA]_0 = 0.1$ mM, $[catalyst]_0 = 50$ mg L$^{-1}$, $[SMX]_0 = 5$ μM, $pH_0 = 6.5$, $T = 25$ °C.

### 3.5 Possible SMX degradation pathways in Co–CN/PAA system

Eight transformation products of SMX were detected in Co–CN/PAA system. Four probable degradation pathways of SMX in Co–CN/PAA system were proposed based on these transformation products, including hydroxylation, nitration, bond cleavage and coupling reaction, as depicted in Fig. 9. Hydroxylation (pathway (1)) might take place on the aniline group of SMX, leading to the generation of product $m/z$ 270.[11,13,18] Amino group on the aromatic ring of SMX and $m/z$ 270 could be further oxidized to generate $m/z$ 284 and $m/z$ 300, respectively (pathway (2)), owing to its electron-rich nature. The formed product $m/z$ 300 might also be produced from product $m/z$ 284 through hydroxylation. The S–N bond in SMX could be broken under the attack of

reactive species ($CH_3C(O)O^{\bullet}$ and $CH_3C(O)OO^{\bullet}$), producing $m/z$ 99 and $m/z$ 158 (pathway (3)).[2] Although $m/z$ 158 was not detected in this study, its formation could not be excluded. Coupling reaction might also occur during SMX degradation in Co–CN/PAA system (pathway (4)), because four dimeric products of SMX were detected. Specifically, coupling reaction might occur between two N-centered radicals both generated from SMX to form $m/z$ 503, while $m/z$ 519 might be formed through the coupling reaction between two N-centered radicals generated from SMX and $m/z$ 270, respectively.[11] The aforementioned N-centered radicals might be produced from the abstraction of hydrogen atom on –$NH_2$ group, because aniline group is an electron-rich moiety, which is easily attacked by radical species.[11,38] Besides, the cleavage of S–N bond in SMX could also
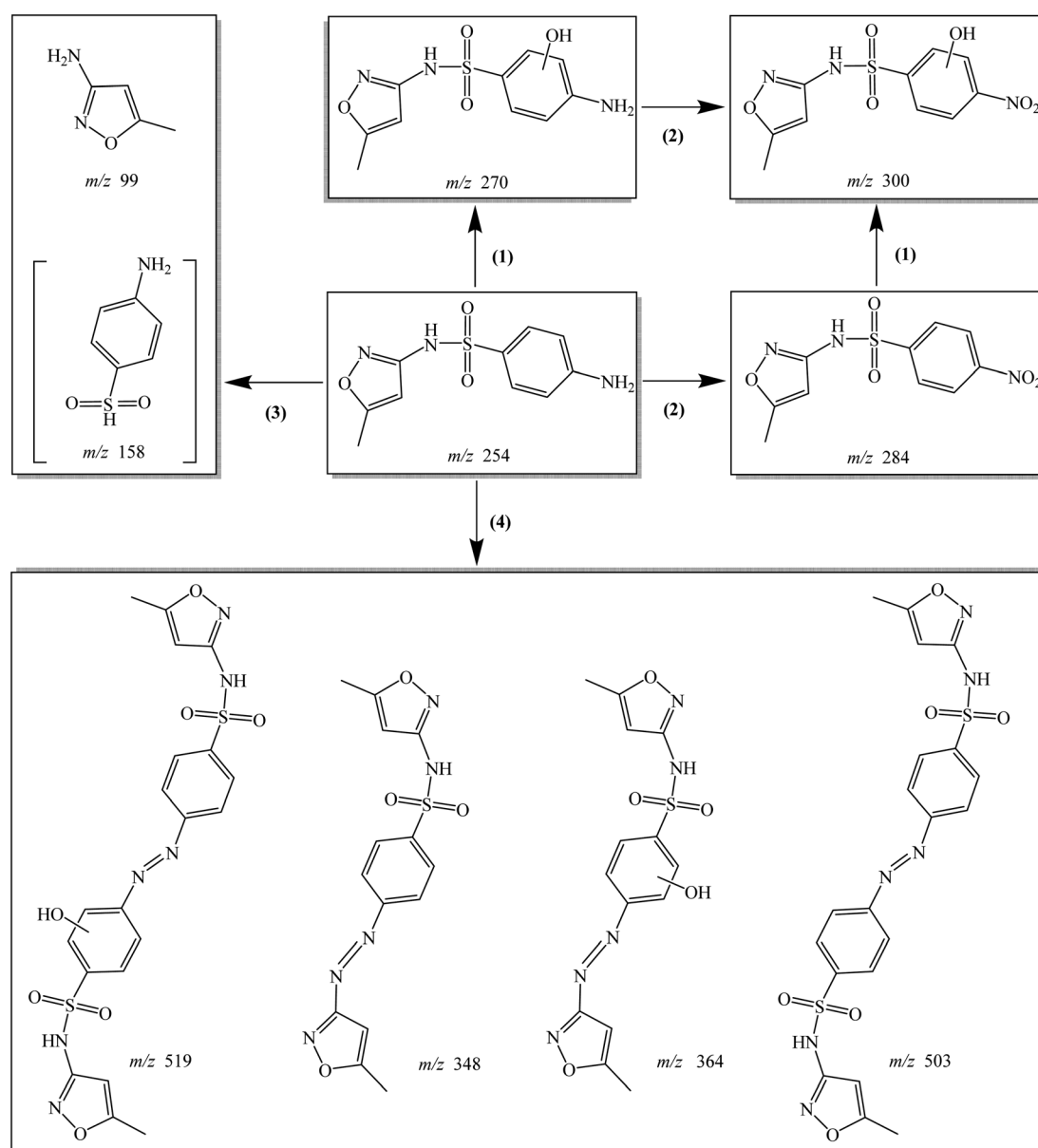


**Fig. 9** Possible degradation pathways of SMX in Co–CN/PAA system: (1) hydroxylation; (2) nitration; (3) bond cleavage; (4) coupling reaction. The product in "[ ]" was not detected in this study.

produce another N-centered radical, which was responsible for the formation of products $m/z$ 348 and $m/z$ 364 through coupling with N-centered radicals generated from SMX and $m/z$ 270, respectively.[11]

## 4. Conclusion

In this work, Co–CN was prepared and applied to activate PAA in degrading SMX. Characterizations (*e.g.*, XRD, XPS, SEM and BET) results revealed that cobalt was distributed evenly in the structure of g-C$_3$N$_4$ through chemical bonding (Co–N bond) in Co–CN. PAA could be activated by the surface $\equiv$Co(II) to produce CH$_3$C(O)O$^{\bullet}$ as well as $\equiv$Co(III). Meanwhile, $\equiv$Co(III) could also react with PAA to produce CH$_3$C(O)OO$^{\bullet}$ and $\equiv$Co(II), leading to the redox cycle of $\equiv$Co(II)/$\equiv$Co(III). These two organic radicals were confirmed to be the dominant reactive species for SMX removal in Co–CN/PAA system by radical scavenging experiments. The near-neutral pH value, higher dosages of PAA and Co–CN as well as higher cobalt doping content in Co–CN were all beneficial to SMX degradation in Co–CN/PAA system. Characterization results of used Co–CN and recycling batch experiments with efficient SMX removal suggested the good stability and reusability of Co–CN. Based on the detected degradation products, hydroxylation, nitration, bond cleavage and coupling reaction were proposed to be the possible transformation pathways of SMX in Co–CN/PAA system.

## Conflicts of interest

There are no conflicts to declare.

## Acknowledgements

## References

1 A. Khan, K. Zhang, A. Taraqqi-A-Kamal, X. Wang, Y. Chen and Y. Zhang, Degradation of antibiotics in aqueous media using manganese nanocatalyst-activated peroxymonosulfate, *J. Colloid Interface Sci.*, 2021, **599**, 805–818.

2 S. Wang, H. Wang, Y. Liu and Y. Fu, Effective degradation of sulfamethoxazole with Fe$^{2+}$-zeolite/peracetic acid, *Sep. Purif. Technol.*, 2020, **233**, 115973.

3 J. Wang and S. Wang, Microbial degradation of sulfamethoxazole in the environment, *Appl. Microbiol. Biotechnol.*, 2018, **102**, 3573–3582.

4 A. Turco, S. Corvaglia, P. P. Pompa and C. Malitesta, An innovative and simple all electrochemical approach to functionalize electrodes with a carbon nanotubes/polypyrrole molecularly imprinted nanocomposite and its application for sulfamethoxazole analysis, *J. Colloid Interface Sci.*, 2021, **599**, 676–685.

5 S. Liu, Y. Fu, G. Wang and Y. Liu, Degradation of sulfamethoxazole by UV/sulfite in presence of oxygen: Efficiency, influence factors and mechanism, *Sep. Purif. Technol.*, 2021, **268**, 118709.

6 S. Wang, G. Wang, Y. Fu and Y. Liu, Sulfamethoxazole degradation by UV-Fe$^{3+}$ activated hydrogen sulfite, *Chemosphere*, 2021, **268**, 128818.

7 Z. Wang, H. Shi, S. Wang, Y. Liu and Y. Fu, Degradation of diclofenac by Fe(II)-activated peracetic acid, *Environ. Technol.*, 2020, DOI: 10.1080/ 09593330.2020.1756926.

8 H. Wang, J. Deng, X. Lu, L. Wan, J. Huang and Y. Liu, Rapid and continuous degradation of diclofenac by Fe(II)-activated persulfate combined with bisulfite, *Sep. Purif. Technol.*, 2021, **262**, 118335.

9 J. Kim, P. Du, W. Liu, C. Luo, H. Zhao and C. Huang, Cobalt/peracetic acid: Advanced oxidation of aromatic organic compounds by acetylperoxyl radicals, *Environ. Sci. Technol.*, 2020, **54**, 5268–5278.

10 R. Zhou, Y. Fu, G. Zhou, S. Wang and Y. Liu, Heterogeneous degradation of organic contaminants by peracetic acid activated with FeCo$_2$S$_4$ modified g-C$_3$N$_4$: Identification of reactive species and catalytic mechanism, *Sep. Purif. Technol.*, 2022, **282**, 120082.

11 Z. Wang, J. Wang, B. Xiong, F. Bai, S. Wang, Y. Wan, L. Zhang, P. Xie and M. R. Wiesner, Application of cobalt/peracetic acid to degrade sulfamethoxazole at neutral condition: Efficiency and mechanisms, *Environ. Sci. Technol.*, 2020, **54**, 464–475.

12 L. Zhang, Y. Liu and Y. Fu, Degradation kinetics and mechanism of diclofenac by UV/peracetic acid, *RSC Adv.*, 2020, **10**, 9907–9916.

13 J. Wang, Y. Wan, J. Ding, Z. Wang, J. Ma, P. Xie and M. R. Wiesner, Thermal Activation of Peracetic Acid in Aquatic Solution: The Mechanism and Application to Degrade Sulfamethoxazole, *Environ. Sci. Technol.*, 2020, **54**, 14635–14645.

14 W. Wu, D. Tian, T. Liu, J. Chen, T. Huang, X. Zhou and Y. Zhang, Degradation of organic compounds by peracetic acid activated with Co$_3$O$_4$: A novel advanced oxidation process and organic radical contribution, *Chem. Eng. J.*, 2020, **394**, 124938.

15 J. Kim, T. Zhang, W. Liu, P. Du, J. T. Dobson and C. Huang, Advanced oxidation process with peracetic acid and Fe(II) for contaminant degradation, *Environ. Sci. Technol.*, 2019, **53**, 13312–13322.

16 X. Zhang, R. Francis, D. Dutton and R. Hill, Decomposition of peracetic acid catalyzed by cobalt(II) and vanadium(V), *Can. J. Chem.*, 1998, **76**, 1064–1069.

17 X. Zhang, R. Francis, D. Dutton and R. Hill, The role of transition metal species in delignification with distilled peracetic acid, *J. Wood Chem. Technol.*, 1998, **18**, 253–266.

18 J. Wang, B. Xiong, L. Miao, S. Wang, P. Xie, Z. Wang and J. Ma, Applying a novel advanced oxidation process of activated peracetic acid by CoFe$_2$O$_4$ to efficiently degrade sulfamethoxazole, *Appl. Catal., B*, 2021, **280**, 119422.

19 X. Zhou, H. Wu, L. Zhang, B. Liang, X. Sun and J. Chen, Activation of peracetic acid with lanthanum cobaltite perovskite for sulfamethoxazole degradation under a neutral pH: The contribution of organic radicals, *Molecules*, 2020, **25**, 2725.

20 L. Cui, S. L. Liu, F. K. Wang, J. Y. Li, Y. H. Song, Y. Sheng and H. F. Zou, Growth of uniform g-C$_3$N$_4$ shells on 1D TiO$_2$ nanofibers *via* vapor deposition approach with enhanced visible light photocatalytic activity, *J. Alloys Compd.*, 2020, **826**, 154001.

21 X. Yang, Z. Tian, Y. Chen, H. Huang, J. Hu and B. Wen, In situ synthesis of 2D ultrathin cobalt doped g-C$_3$N$_4$ nanosheets enhances photocatalytic performance by accelerating charge transfer, *J. Alloys Compd.*, 2021, **859**, 157754.

22 Y. Wang, B. Y. Gao, Q. Y. Yue and Z. N. Wang, Graphitic carbon nitride (g-C$_3$N$_4$)-based membranes for advanced separation, *J. Mater. Chem. A*, 2020, **8**, 19133–19155.

23 W. Oh, V. Chang, Z. Hu, R. Goei and T. Lim, Enhancing the catalytic activity of g-C$_3$N$_4$ through Me doping (Me = Cu, Co and Fe) for selective sulfathiazole degradation *via* redox-based advanced oxidation process, *Chem. Eng. J.*, 2017, **323**, 260–269.

24 X. Wang, X. Chen, A. Thomas, X. Fu and M. Antonietti, Metal-containing carbon nitride compounds: A new functional organic-metal hybrid material, *Adv. Mater.*, 2009, **21**, 1609–1612.

25 M. Xie, J. Tang, L. Kong, W. Lu, V. Natarajan, F. Zhu and J. Zhan, Cobalt doped g-C$_3$N$_4$ activation of peroxymonosulfate for monochlorophenols degradation, *Chem. Eng. J.*, 2019, **360**, 1213–1222.

26 Y. Shang, X. Chen, W. Liu, P. Tan, H. Chen, L. Wu, C. Ma, X. Xiong and J. Pan, Photocorrosion inhibition and high-efficiency photoactivity of porous g-C$_3$N$_4$/Ag$_2$CrO$_4$ composites by simple microemulsion-assisted co-precipitation method, *Appl. Catal., B*, 2017, **204**, 78–88.

27 I. Rabani, R. Zafar, K. Subalakshmi, H. S. Kim, C. Bathula and Y. S. Seo, A facile mechanochemical preparation of Co$_3$O$_4$@g-C$_3$N$_4$ for application in supercapacitors and degradation of pollutants in water, *J. Hazard. Mater.*, 2021, **407**, 124360.

28 K. Zhang, X. Zhou, P. Du, T. Zhang, M. Cai, P. Sun and C. Huang, Oxidation of beta-lactam antibiotics by peracetic acid: Reaction kinetics, product and pathway evaluation, *Water Res.*, 2017, **123**, 153–161.

29 L. Xu and J. Wang, Magnetic nanoscaled Fe$_3$O$_4$/CeO$_2$ composite as an efficient fenton-like heterogeneous catalyst for degradation of 4-chlorophenol, *Environ. Sci. Technol.*, 2012, **46**, 10145–10153.

30 L. Zhang, J. Chen, Y. Zhang, Z. Yu, R. Ji and X. Zhou, Activation of peracetic acid with cobalt anchored on 2D sandwich-like MXenes (Co@MXenes) for organic contaminant degradation: High efficiency and contribution of acetylperoxyl radicals, *Appl. Catal., B*, 2021, **297**, 120475.

31 F. Guo, W. Shi, C. Zhu, H. Li and Z. Kang, CoO and g-C$_3$N$_4$ complement each other for highly efficient overall water splitting under visible light, *Appl. Catal., B*, 2018, **226**, 412–420.

32 J. Mu, J. Li, X. Zhao, E. Yang and X. Zhao, Cobalt-doped graphitic carbon nitride with enhanced peroxidase-like activity for wastewater treatment, *RSC Adv.*, 2016, **6**, 35568–35576.

33 H. Li, J. Qian and B. Pan, N-coordinated Co containing porous carbon as catalyst with improved dispersity and stability to activate peroxymonosulfate for degradation of organic pollutants, *Chem. Eng. J.*, 2021, **403**, 126395.

34 X. Huang, N. Zhu, F. Mao, Y. Ding, S. Zhang, F. Li, H. Liu and P. Wu, Novel Au@C modified g-C$_3$N$_4$ (Au@C/g-C$_3$N$_4$) as efficient visible-light photocatalyst for toxic organic pollutant degradation: Synthesis, performance and mechanism insight, *Sep. Purif. Technol.*, 2020, **252**, 117485.

35 H. Li, C. Shan and B. Pan, Fe(III)-doped g-C$_3$N$_4$ mediated peroxymonosulfate activation for selective degradation of phenolic compounds *via* high-valent iron-oxo species, *Environ. Sci. Technol.*, 2018, **52**, 2197–2205.

36 L. Wang, X. Guo, Y. Chen, S. Ai and H. Ding, Cobalt-doped g-C$_3$N$_4$ as a heterogeneous catalyst for photo-assisted activation of peroxymonosulfate for the degradation of organic contaminants, *Appl. Surf. Sci.*, 2019, **467**, 954–962.

37 M. Cai, P. Sun, L. Zhang and C. Huang, UV/peracetic acid for degradation of pharmaceuticals and reactive species evaluation, *Environ. Sci. Technol.*, 2017, **51**, 14217–14224.

38 E. N. Step, N. J. Turro, M. E. Gande and P. P. Klemchuk, Mechanism of polymer stabilization by hindered-amine light stabilizers (HALS). Model investigations of the interaction of peroxy radicals with HALS amines and amino ethers, *Macromolecules*, 1994, **27**, 2529–2539.